한국지반공학회논문집 제22권 6호 2006년 6월 pp. 27 ~ 40

Variation of Earth Pressure Acting on Cut-and-Cover Tunnel Lining with Settlement of Backfill

되메움토의 침하에 따른 개착식 터널 라이닝에 작용하는 토압의 변화

Bautista, F. E.[1] 펄디난드 이. 바우티스타 Park, Lee-Keun[2] 박 이 근
Im, Jong-Chul[3] 임 종 철 Lee, Young-Nam[4] 이 영 남

요 지

개착식 터널라이닝의 파괴 원인은 물리적 요인과 공학적 요인으로 나눌 수 있다. 물리적 요인으로서는 재료특성, 보강재 부식 등이 있으며, 공학적 요인은 수압과 교통진동 등이 있다. 본 연구에서는 공학적 요인 중 부가하중 즉, 공사를 완료한 뒤에 라이닝의 변형 및 파괴를 유발하는 증가 토압에 초점이 맞추어져 있다. 증가 토압은 되메움토의 다짐 불량, 자중 및 강우에 의한 침하, 교통하중에 의한 진동 등이 원인이 되어 발생한다. 본 연구는 모래 지반에 1.0D~1.50D 깊이에 개착식으로 시공하는 원형의 강성 터널에 작용하는 토압에 관한 것으로 진동다짐의 영향을 모형실험에서 충분히 반영하기 위하여 100Hz의 진동주파수를 사용하였다. 본 연구에서는 개착식 터널 라이닝에 작용하는 토압과 주변 지반의 변형 양상을 파악하고 기존 토압 계산 공식을 검토하기 위해 실내 터널모형실험을 실시하였으며, 개착식 터널 라이닝에 작용하는 측정 토압과 토압공식에 의해 산출한 토압을 비교·분석하여 기존 공식에 대한 안전율을 제시하였다.

Abstract

Damage of cut-and-cover tunnel lining can be attributed to physical and mechanical factors. Physical factors include material property, reinforcement corrosion, etc. while mechanical factors include underground water pressure, vehicle loads, etc. This study is limited to the modeling of rigid circular cut and cover tunnel constructed at a depth of 1.0~1.5D in loose sandy ground and subjected to a vibration frequency of 100 Hz. In this study, only damages due to mechanical factors in the form of additional loads were considered. Among the different types of additional, excessive earth pressure acting on the cut-and-cover tunnel lining is considered as one of the major factors that induce deformation and damage of tunnels after the construction is completed. Excessive earth pressure may be attributed to insufficient compaction, consolidation due to self-weight of backfill soil, precipitation and vibration caused by traffic. Laboratory tunnel model tests were performed in order to determine the earth pressure acting on the tunnel lining and to investigate the applicability of existing earth pressure formulas. Based on the difference in the monitored and computed earth pressure, a factor of safety was recommended. Soil deformation mechanism around the tunnel was also presented using the picture analysis method.

Keywords : Cut and cover tunnel, Earth pressure, Tunnel lining, Tunnel model test

1 Member, Doctor Course-Pusan National Univ. Researcher of RIIT-PNU, denndenn@hotmail.com
2 Member, Ph.D., Researcher of RIIT, Pusan National Univ., theman4you@korea.com
3 Member, Ph.D., Prof., Dept. of Civil Engrg., Pusan National Univ., imjc@pusan.ac.kr
4 Member, Ph.D., Director, Research & Dev't Department, Hyundai Construction

* 본 논문에 대한 토의를 원하는 회원은 2006년 12월 31일까지 그 내용을 학회로 보내주시기 바랍니다. 저자의 검토 내용과 함께 논문집에 게재하여 드립니다.

1. Introduction

In spite of the continuous development of more sophisticated tunnelling methods, cut-and-cover method is still used since it is the most economical and easy to apply. It is also used in cases wherein other methods are not feasible, like shallow tunnels and mountain tunnel portals. Even though it is the oldest method still a lot of problems are encountered in its use, problems that can be attributed to design and construction. In this type of tunnel construction, the compaction of the backfill material is the most important process, especially the compaction of backfill soil on both sides of the tunnel. Assuming that the backfill material is properly compacted, several months or years after the construction is completed the backfill has the tendency to consolidate due to self-weight, precipitation and vibration caused by traffic. In the process, the tunnel is subjected to excessive earth pressure that causes the deformation and cracking of the tunnel lining. These are classified as mechanical factors that cause tunnel damage. Damages can be also be attributed to physical factors such as material properties, reinforcement corrosion, etc. but in this study only damages due to mechanical factors in the form of additional loads will be considered.

Since actual testing is difficult and very expensive, tunnel model tests with shallow soil cover of 1.0D~ 1.50D (D is the tunnel diameter) were selected for this study. A tunnel model which is a simple reduction of the actual structure at a scale of 1:20 was installed in a plane strain soil tank and was subjected to a vibration frequency of 100 Hz.

When it comes to the design process, there is also a possibility that existing earth pressure formulas has the tendency to underestimate the earth pressure acting on the tunnel lining. Due to these reasons there is a necessity to investigate the earth pressure acting on the cut and cover tunnel lining. Earth pressure monitored from the laboratory model tests was compared with earth pressure computed using Terzaghi (1956), Bierbäumer (1913), Marston-Spangler's Ditch and Projecting Type (Spangler, 1948) and Terzaghi's Modified Earth Pressure Formula in order to determine the most appropriate earth pressure computation method. Depending on the earth pressure method, a factor of safety was recommended and the behaviour of soil around the tunnel was investigated.

2. Case History on Cut and Cover Tunnel in Sandy Ground

Up to the present there has been a lot of local and international case histories of tunnel model tests performed. Depending on the objective of the model test, different testing methods and conditions were applied. Different soil tank and modelling materials were also used. Different ground modeling materials such as sands (Konig et al., 1991; Adachi et al., 1991; Komiya et al., 2000; Ko et al., 1996; Park, 2003; Im et al., 2002), clays (Britto, 1979) and other materials like aluminum rods (Yuasa, 1988) were used. Tests were performed either in soil tanks of different shapes and sizes or in tests pits. In most cases rectangular soil tanks were used (Adachi et al., 1991; Nakai et al., 1999; Ko et al., 1996; Park, 2003; Im et al., 2002). In particular cases tests were also performed in circular tanks (Britto, 1979) and underground test pits (Yoo, 1997). Different materials were also used in the tunnel model, such as aluminun (Adachi et al., 1991) stainless steel (Park, 2003; Kim et al., 2002), concrete (Lee et al., 1998; Yoo, 1997) and other materials. The monitored parameters also varied from tunnel deformation, surface settlement, underground pressure, etc.

There were also some model tests of cut and cover tunnel in sandy soils performed locally. Lee et al. (1998) performed a model test to determine the mechanical behaviour and cracking characteristics of tunnel lining; Kim (1999) performed a study to determine the earth pressure acting on a box tunnel. Kim et al. (2002) used the shaking table apparatus to analyze the seismic performance of cut-and-cover tunnel, and Kim (2004) performed a tunnel model tests to determine the reduction method for earth pressure acting on the lining of a cut and cover tunnel.

3. Tunnel Model Test Equipment and Testing Method

3.1 Test Equipment

The plane strain model test was made possible through the use of equipments such as : ① plane strain soil tank (Ko et al., 1996; Im et al., 2000; Park, 2003), ② cut slope model, ③ transverse tunnel model, ④ model soil laying apparatus, ⑤ vibratory compaction apparatus, ⑥ load cell and ⑦ deformation analysis program. The specifications of these equipments are presented below.

3.1.1 Plane Strain Soil Tank

The plane strain soil tank used in this study has an internal dimension of 720 mm (H) × 1490 mm (L) × 400 mm (W) and an internal volume of $V = 0.429m^3$. The soil tank is supported by 2 springs and 4 braces. The braces prevent the movement of the soil tank during soil preparation and are unfastened before the soil is subjected to vibration generated by the motor (vibrator) installed beneath the soil tank. The front and rear portions of the soil tank are made of acrylic plate reinforced with steel bars on the outside. Grid printed acetate was applied on the acrylic plates to reduce friction when the targets are installed. The grid on the acetate also serves as a guide in the target installation and soil laying process. The plane strain soil tank diagram is shown in Fig. 1 and Photo 1.

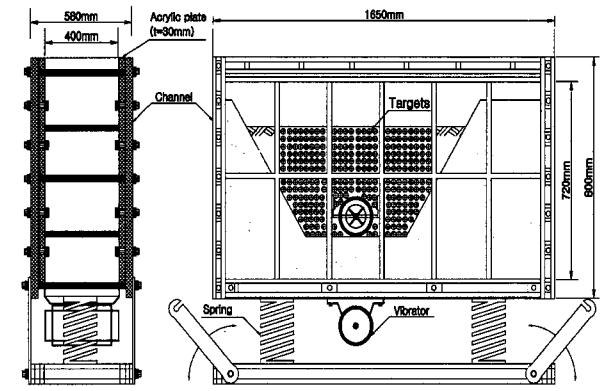

Fig. 1. Plane Strain Soil Tank Diagram

3.1.2 Cut Slope Model

Cut slope model made of plyboard was installed at an angle of 45° on both sides of the tunnel at a distance (G) 1D from the center of the tunnel. The friction of cut slope was considered through the installation of sand paper (#100, #400 and acetate) on the slope surface. The cut slope and tunnel model covered with sandpaper are shown in Photo 2.

3.1.3 Transverse Tunnel Model

The transverse tunnel model used in this study is made of 10 mm stainless steel at a scale of 1:20. It has a diameter (D) of 180 mm and is made of 8 segments. The bi-directional load cell is installed on each segment in order to measure the earth pressure acting on the crown, shoulder and sides of the tunnel. Load cell installation layout is shown in Fig. 2 and a picture of the installed

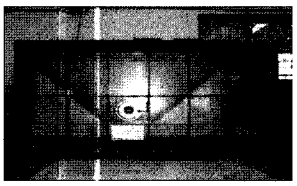

Photo 1. Plane Strain Soil Tank

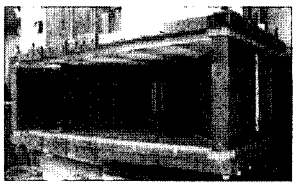

Photo 2. Cut slope and tunnel model

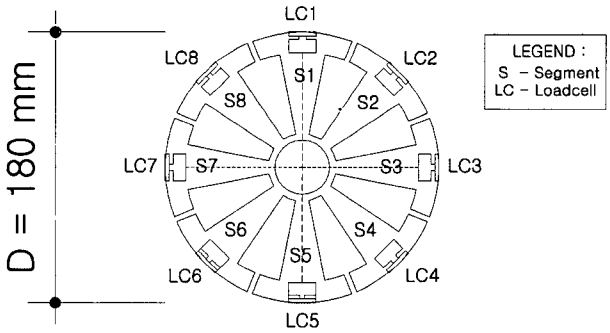

Fig. 2. Load cell Installation

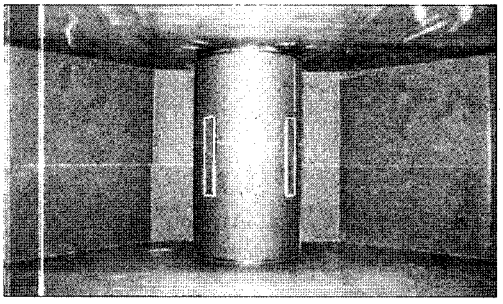

Photo 3. Transverse tunnel model

transverse tunnel model is shown in Photo 3.

3.1.4 Model Soil Laying Apparatus

Backfill soil was modeled using Sand Drop Method wherein the sand is dropped from a slot at a constant height and velocity. To ensure that the sand is layed at a state closes to the minimum dry density ($1.378 g/cm^3$) of Jumunjin Standard Sand, handheld slot made of acrylic plates with an opening of 3 mm was used. A drop height of 3~5 cm was selected from the variation of relative density with the drop height and drop velocity shown in Figure 2.5 and Figure 2.6. Using this slot, loose sand with relative density of 38.9% was produced. The diagram of the handheld slot used in this study is shown in Fig. 3 and Photo 4. In this study the 90~95% compaction which is implemented in the field was not considered in order to obtain a large range of soil density variation.

3.1.5 Deformation Monitoring Device

In this study, the soil in the tank is subjected to vibration for a period of 10 minutes which makes the use of dial gauges difficult. There is a possibility that the dial gauge will be disconnected and damaged during the test. Instead, strings with weights attached on one end and lowered from an aluminum channel section placed longitudinally on the top of the soil tank was used to measure the initial surface level and final surface settlement. Markings are made on the strings lowered from the aluminum channel section onto the soil surface. The measured displacements were used in the calculation of the model soil's volume and density before and after the test. Surface monitoring device used in this test is shown in Photo 5.

In spite of its tedious installation, soil displacement monitoring using targets was selected. The behaviour of

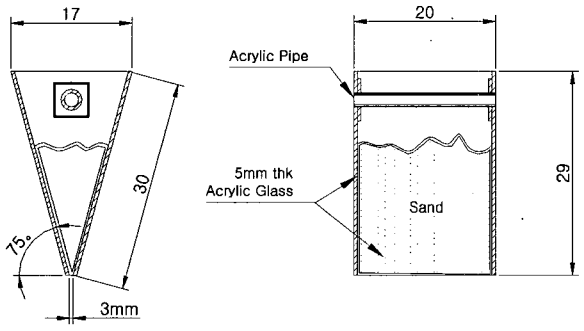

Fig. 3. Handheld Slot Diagram

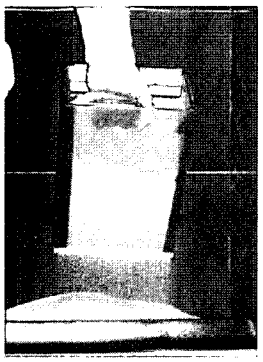

Photo 4. Handheld Slot

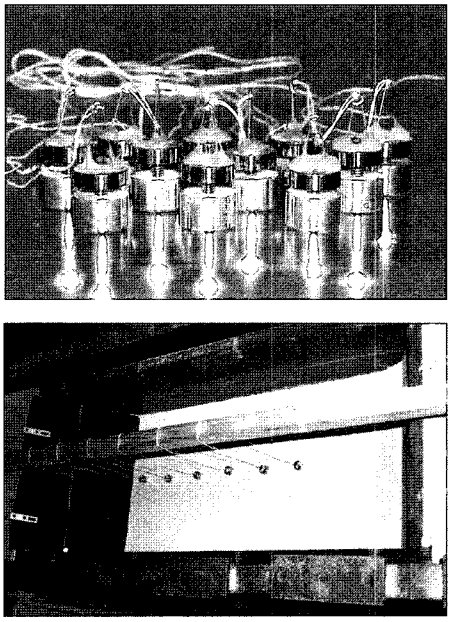

Photo 5. Surface settlement monitoring apparatus

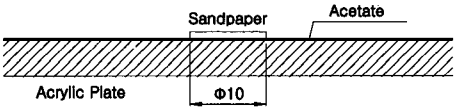

Fig. 4. Targets

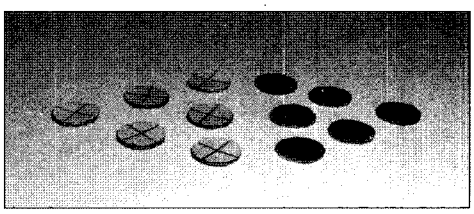

Photo 6. Targets

soil was monitored using 1 cm diameter targets with cross hair in front and sandpaper on the rear end. Targets were installed at 2.5 cm × 2.5 cm square interval on the front acrylic plate coated and covered with acetate. This is shown in Fig. 4 and Photo 6.

3.1.6 Vibratory Compaction Device

A vibrator (motor) is installed under the plane strain soil tank to compact the soil (refer to Fig. 1). The control box controls the overall function of the vibrator. As shown in Fig. 5 and Photo 7, the control box houses the analog frequency controller, timer and automatic shutdown switch. Since the exact frequency and vibration time can be accurately controlled, the tests in this study were performed at uniform condition.

3.2 Modelling Materials

Jumunjin Standard Sand was used in the modelling of the soil. The physical and mechanical properties of Jumunjin Standard Sand determined through laboratory tests are presented below.

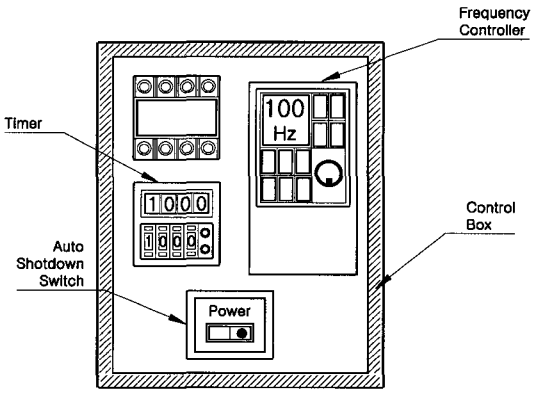

Fig. 5. Control Box Diagram

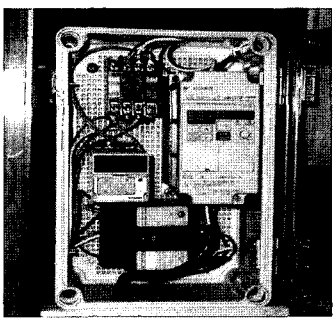

Photo 7. Vibratory Compactor Control Box

3.2.1 Physical Properties

A water content (w) of 0.3% was obtained from the naturally dried state. Physical properties of Jumunjin Standard Sand is tabulated in Table 1. Based on the result of the particle size analysis of the Jumunjin Standard Sand, it was determined that the particle sizes range from 0.40~0.85. Other particle diameter information obtained from the particle size analysis is tabulated in Table 2.

3.2.2 Variation of Density with the Soil Laying Apparatus

Handheld slot was used in the preparation of the model soil. When sand is prepared from a slot with a free fall height, then the quantity of sand spread at a designated period of time and density of the model soil is dependent on the slot opening. At a constant drop height the density of sand will also vary with the speed of sand drop. In order to determine the variation of sand density with the drop height and speed of drop height, Sand Drop Height Density Test and Sand Drop Velocity Density Test were performed. The variation of the density of Jumunjin Standard Sand with the drop height and drop velocity is shown below.

① Sand Drop Height Density Test

Sand drop height density tests were performed using

Table 1. Physical Properties

Physical Properties	Symbol	Unit	Value
Max. dry density	γ_{dmax}	g/cm^3	1.652
Min. dry density	γ_{dmin}	g/cm^3	1.378
Max. void ratio	$e_{\max}$	-	0.923
Min. void ratio	$e_{\min}$	-	0.604
Water content	w	%	0.300
Specific Gravity	G_s	-	2.650

Table 2. Particle Size Information

Physical Properties	Symbol	Unit	Value
Effective Diameter	D_{10}	mm	0.443
Average Diameter	D_{50}	mm	0.595
Maximum Diameter	$D_{\max}$	mm	0.850
Curvature Coefficient	C_g	-	0.912
Uniformity Coefficient	C_u	-	1.402

a slot type sand laying apparatus on several density cans at constant speed. The variation of the density of sand at different drop heights under constant sand laying speed was determined and plotted in Fig. 8. It can be seen in this figure that even at constant sand laying speed, the density of Jumunjin Standard Sand varies with the drop height.

Based on this graph, the variation of the density of sand with the drop height was determined. Since the model soil must be prepared at a loose state, a drop height within the shaded area must be selected. A drop height of 3～5 cm was selected for the handheld slot. This drop height produced a model ground with a density of 1.449 g/cm^3 to 1.467g/cm^3.

② Sand Laying Velocity Density Test

Sand laying velocity density tests were performed to determine the effect of sand drop velocity on the density of Jumunjin Standard Sand. The results of these tests are shown in Fig. 9. Since the model soil must be prepared as loosely as possible, an average sand laying velocity 25$cm/\sec$ was selected from this graph. The sand laying velocity was maintained during all the tests using the hand held slot with slot opening of 3 mm×190 mm.

3.2.3 Mechanical Properties

Direct Shear Test, Standard Compression Test, and Plane Strain Compression Test were performed to determine the shear resistance angle of Jumunjin Standard Sand. The difference in shear resistance angle obtained from each method was determined and presented in Table 3 (Park 2003).

3.3 Monitoring Equipment

3.3.1 Earth Pressure Monitoring Device

In this study, a bi-directional load cell was installed on each segment of the 8-segment transverse tunnel model to monitor the earth pressure. The surface of the bi-directional load cell is covered with Sandpaper #100 (Refer to Photo 2 and Photo 3). The correction coefficient test was performed in order to determine whether there is coupling effect on the vertical and horizontal direction of the load cell. Based on the test result, the correction coefficient was determined and was applied to the test results obtained from the tunnel model test. It can be seen

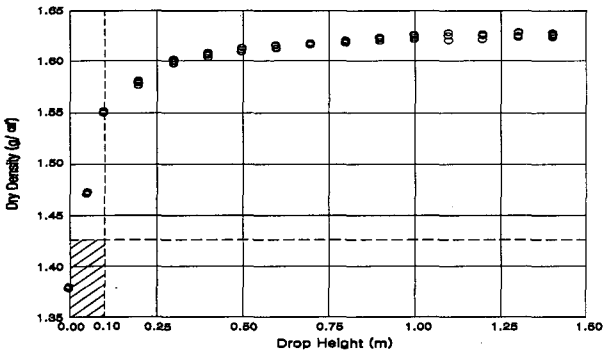

Fig. 8. Dry density variation w/ drop height

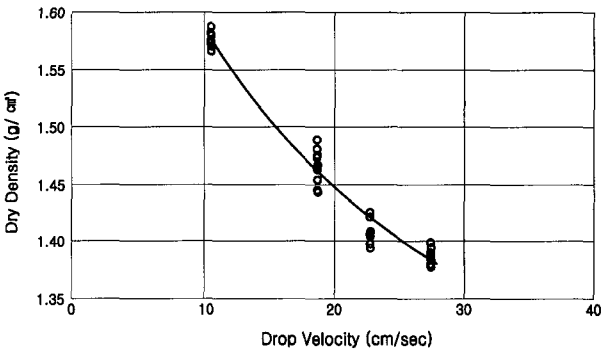

Fig. 9. Dry density variation w/ drop velocity

Table 3. Standard Triaxial Compression Test Results

Parameters	Test Types																	
	Direct Shear Test								Standard Triaxial Compression Test				Plane Strain Compression Test					
Number	1	2	3	4	5	6	7	8	1	2	3	4	1	2	3	4	5	6
γ_d (g/cm^3)	1.38	1.47	1.52	1.56	1.57	1.60	1.63	1.65	1.39	1.45	1.55	1.61	1.38	1.41	1.42	1.46	1.58	1.65
Dr (%)	0	36.9	57.0	70.7	74.4	84.3	93.8	98.2	6.9	29.9	66.9	86.9	0	11.6	15.8	31.9	77.1	98.5
ϕ_{TCT} (°)	31.2	33.0	35.0	33.7	38.0	39.2	41.1	42.0	31.2	33.4	36.5	41.3	36.4	35.8	36.8	39.6	46.1	51.1

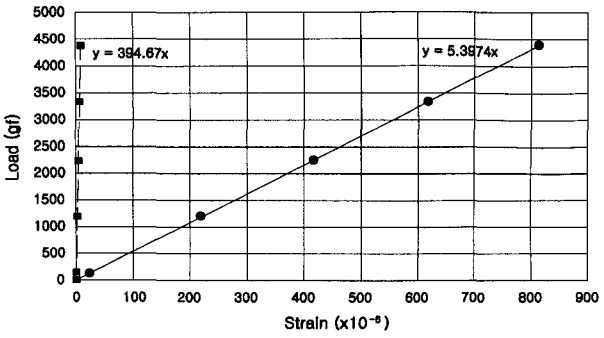

Fig. 10. Coupling of Bi-directional Load Cell

in Fig. 10, that there is no coupling effect.

3.3.2 Earth Pressure Recording Device

The UCAM-10A strain monitoring device was used to measure the horizontal and vertical loads acting on the load cell. The earth pressure before and after vibration was monitored and printed-out.

3.3.3 Deformation Analysis Program

Deformation analysis for laboratory model test introduced by Im et al. (1992), was used to analyze the behaviour of soil around the tunnel based on the pictures taken before and after vibration. The picture taken during the laboratory model test was interpreted using Microstation and analyzed using Deformation Analysis for Laboratory model Test introduced - DALT (Park 2003). Through this analysis the soil behaviour was determined.

3.4 Test Method

The earth pressure acting on a cut-and-cover tunnel with soil covers of 1.0D~1.5D at a slope angle of 45° was determined through model tests. The relationship between earth pressure and other factors such as slope roughness was also investigated.

3.4.1 Types of Tests

3.4.1.1 Model Tests with Varying Soil Cover

Model tests representing the tunnel structure with varying soil covers were performed. The most conservative slope angle of 45° used in actual construction was selected for this study. The behaviour of the soil and

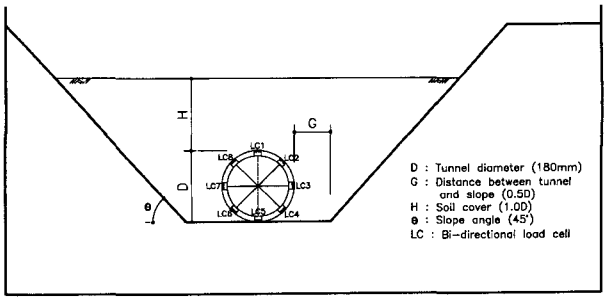

< FRONT ELEVATION >

Fig. 11. Test Diagram for 1.0D Soil Cover

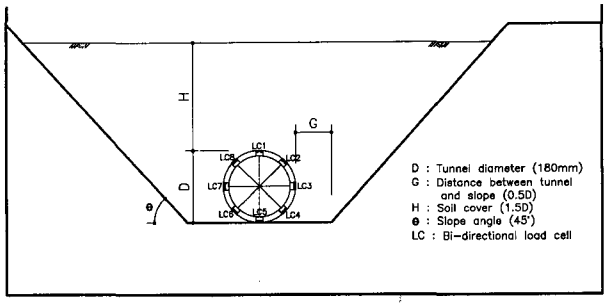

< FRONT ELEVATION >

Fig. 12. Test Diagram for 1.50D Soil Cover

stress condition around the tunnel together with the surface settlement were investigated. The depth of soil cover is represented by the tunnel diameter (D). The test when it comes to soil cover is divided into 1.0D and 1.5D. The schematic diagram of the model test is presented in Fig. 11 and Fig. 12.

3.4.1.2 Model Tests with Varying Slope Roughness

To determine the effect of slope roughness on the soil behaviour, earth pressure and other geometric factors, 2 types of sand paper (#100 and #400) and acetate were used to model the roughness of the slope surface.

3.4.2 Test Sequence

This study was performed based on the sequence shown in Fig. 13.

3.4.3 Vibration Frequency

During the preliminary tests, frequencies of 50 Hz, 75 Hz and 100 Hz were used at various duration of time. A frequency of 100 Hz with a vibration period of 10 minutes was selected from the preliminary test since at

this frequency up to a period of about 10 minutes there was a rapid increase in density. After a period of 10 minutes the increase in density was very minimal and becomes constant. The variation of soil density with frequency and time is shown in Fig. 14.

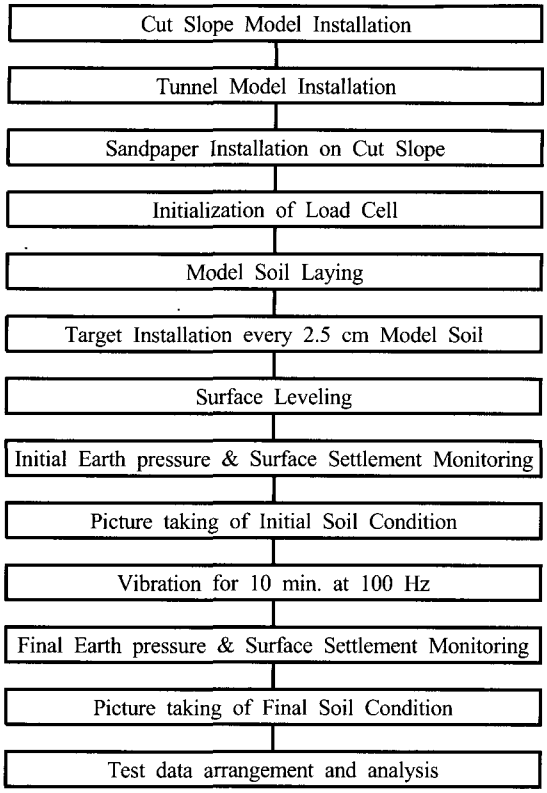

Fig. 13. Test Sequence

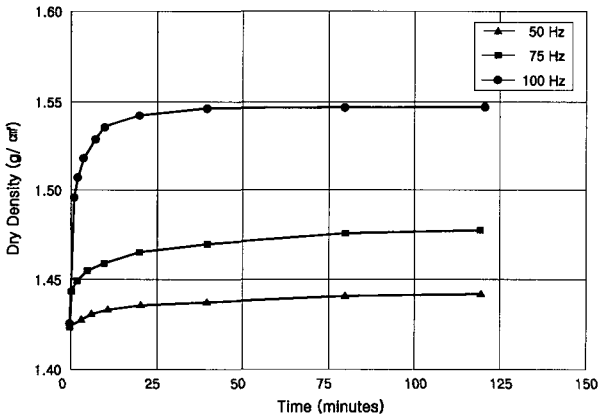

Fig. 14. Variation of density with vibration frequency

4. Result of the Tunnel Model Test

Even though 8 load cells were installed on the eight segments of the tunnel lining only readings from 5 loadcells located at the crown, shoulders and sidewalls were considered. The monitored earth pressure before and after vibration are presented in Table 4.

Fig. 15 shows the earth pressure acting on the tunnel lining after vibration for the four types of test. It can be seen in the figure that the earth pressure at the tunnel crown for 1.50D-100 is about 40% greater than 1.0D-100, up to about 36% greater at the shoulder and up to about 36% at the sidewall.

In the case of excavated tunnel, the earth pressure acting on a 1.0D tunnel may be bigger than 1.50D tunnel but in the case of cut and cover tunnels the earth pressure acting on a 1.50D is greater than that of a 1.0D tunnel.

4.1 Analysis of Earth Pressure Around the Tunnel

The earth pressures around the tunnel (1.0D-100, 1.5D-100, 1.5D-400 & 1.5D-ACE) were monitored, compared and analyzed. The monitored earth pressure for each test was compared with the computed earth pressure using Terzaghi's Earth Pressure Formula, Bierbäumer's Formula, Marston- Spangler's Ditch Type and Projecting Type Formula and Terzaghi's Modified Earth Pressure Formula. The ratio between the monitored and computed earth pressure will serve as the factor of safety to be used in the earth pressure computation for tunnel lining design of a Cut and Cover Tunnel.

Table 4. Variation of Earth Pressure with Soil Cover

Load Cell Location		Earth Pressure Before Vibration (gf/cm^2)				Earth Pressure After Vibration (gf/cm^2)			
		1.00D-100	1.50D-100	1.50D-400	1.50D-ACE	1.00D-100	1.50D-100	1.50D-400	1.50D-Ace
Crown		41.110	50.770	49.126	50.154	57.142	96.608	90.236	66.803
Shoulder	Right	15.924	24.702	22.456	22.252	19.394	30.418	33.072	37.972
	Left	18.578	21.232	20.619	20.007	25.723	30.214	32.664	33.276
Sidewall	Right	16.740	31.235	37.768	38.788	20.415	19.803	35.114	25.110
	Left	15.515	30.214	32.868	36.747	22.456	35.318	47.159	62.062

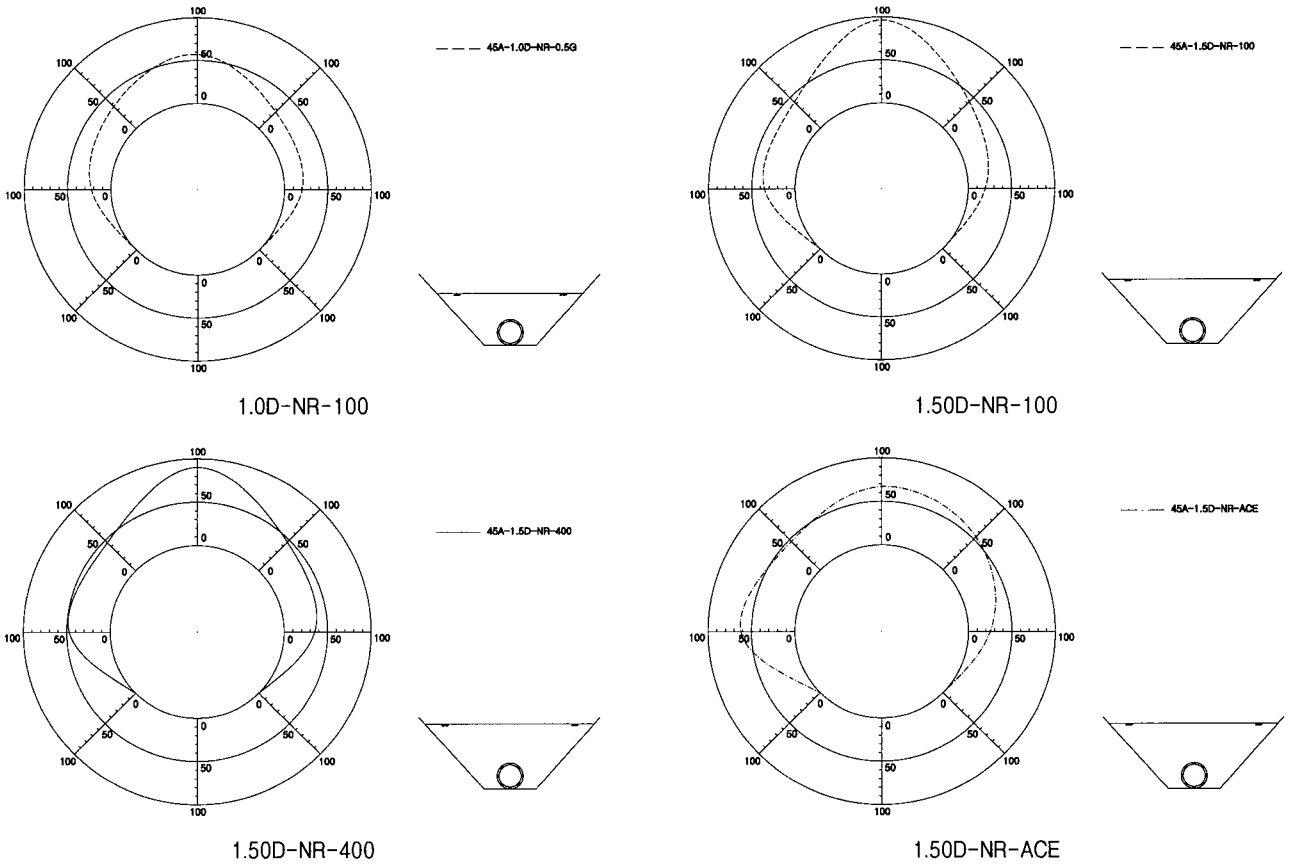

Fig. 15. Variation of Earth Pressure Acting on Tunnel Lining (After Vibration)

Table 5. Dry Density and Monitored Earth Pressure Before and After Vibration

Tests Type	Initial Dry Density, γ_{iave} (gf/cm^3)	Final Dry Density γ_{fave} (gf/cm^3)	Monitored Initial Earth Pressure (gf/cm^2)	Comp. Initial Earth Pressure $\gamma_{iave} \times H$ (gf/cm^2)	Monitored Final Earth Pressure (gf/cm^2)	Comp. Final Earth Pressure $\gamma_{fave} \times H$ (gf/cm^2)
1.00D-100	1.467	1.578	41.11	26.40	57.14	28.40
1.50D-100	1.464	1.529	50.77	39.53	96.61	41.28
1.50D-400	1.452	1.524	49.13	39.20	90.24	41.15
1.50D-ACE	1.449	1.515	50.15	39.12	66.80	40.91

The earth pressures acting on the tunnel before and after vibration were measured using the loadcell installed on the tunnel segments. After vibration a relative density of 66.9% was attained. The monitored and computed earth pressures and their corresponding dry density before and after vibration are presented in Table 5. It can be seen in this table that the earth pressure computed using $\sigma_v = \gamma_{ave} H$ is a lot smaller than the monitored values. Here H is the soil cover.

4.1.1 Vertical Earth Pressure Computation

Computation of earth pressure was performed using the following conditions: $D = 18cm$, $H = 18cm(1.0D)$ $H = 27cm(1.5D)$, $\phi = 36.5^\circ$, $K = 1 - \sin\phi = 1 - \sin 36.5 = 0.405$ and $D_r = 66.9\%$. Earth pressure computed using different earth pressure formulas is shown in Table 6.

Table 7 shows the ratio between the monitored and computed earth pressure using different formulas. For model tests with 1.0D soil cover, the ratio between the monitored and computed values ranged from 1.47~2.67. The smallest value of 1.47 was obtained using Marston-Spangler's Projecting Type earth pressure formula. For model tests with 1.50D soil cover, a ratio of 1.01~3.55 was obtained. Among all the model tests with 1.50D soil

Table 6. Earth pressure computed using different earth pressure formulas

Test Type	Computed Earth Pressure (gf/cm^2)				
	Terzaghi's Formula	Bierbäumer's Formula	Marston- Spangler's Formula		Terzaghi's Mod. Formula
			Ditch Type	Projecting Type	
1.00D-100	24.59	28.29	21.39	38.96	38.96
1.50D-100	33.29	41.07	27.23	66.93	66.92
1.50D-400	33.08	40.93	27.14	66.71	67.56
1.50D-ACE	33.29	40.69	26.98	66.32	67.14

Table 7. Ratio between the monitored and computed earth pressure

Test Type	Earth Pressure Formulas				
	Terzaghi's Formula	Bierbäumer's Formula	Marston- Spangler's Formula		Terzaghi's Mod. Formula
			Ditch Type	Projecting Type	
1.00D-100	2.32	2.02	2.67	1.47	1.58
1.50D-100	2.90	2.35	3.55	1.44	2.67
1.50D-400	2.73	2.20	3.32	1.35	2.50
1.50D-ACE	2.00	1.64	2.48	1.01	1.85

Table 8. Monitored and Computed Horizontal Earth Pressure on the sidewalls

Test Type	Dry Density γ_{ave} (gf/cm^3)	Static Earth Pressure (gf/cm^2)	Ave. Mon. Earth Pressure (gf/cm^2)	Computed Earth Pressure (gf/cm^2)	Ratio (Mon. & Comp. Earth Pressure)
1.00D-100	1.578	10.84	21.14	17.28	1.24
1.50D-100	1.529	13.98	31.64	22.29	1.42
1.50D-400	1.5.24	13.94	39.50	22.22	1.78
1.50D-ACE	1.515	13.85	40.93	22.09	1.85

cover, the smallest value was obtained from the acetate covered slope (1.50D-ACE) wherein the monitored and computed earth pressure was almost equally followed.

If we consider the earth pressure monitored on the tunnel crown, it can be seen that the earth pressure computed using Marston-Spangler's Projecting Type Formula should be multiplied by a safety factor of 1.3~1.5 when used in design of tunnels with depths less than 1.50D.

4.1.2 Horizontal Earth Pressure Computation

$\sigma_{ho(m)} > \sigma_{ho} > \sigma_{ha}$ relationship can be established based on the values in Table 8.

4.2 Picture Analysis

Pictures of the model test were taken before, during and after a test to determine the behaviour of soil around the tunnel. The pictures were interpreted using Micro-station and analyzed using the DALT (Park, 2003).

4.2.1 Behaviour of Soil around the Cut and Cover Tunnel

4.2.1.1 Variation in Soil Cover

Fig. 16 (a) shows the soil displacement contour diagram for model tests with 1.0D and 1.50D soil cover. The soil displacement contour diagram was redrawn in Fig. 16 (b) to clearly show the behaviour of soil around the tunnel. If we were to observe the soil displacement contour diagram in the vertical direction in Fig. 16 (b), it can be seen that the soil behaviour is similar to the displacement mechanism of Marston-Spangler's Projecting Type earth pressure theory. Furthermore, the soil displacement of soil mass above the tunnel is remarkably smaller compared to the displacement of the soil mass around the tunnel lining. From this figure, it can be concluded that the principle of load relaxation and arching effect considered in tunnel excavation is not

applicable.

4.2.1.2 Variation in Slope Roughness

Soil displacement contour diagram for model tests with varying slope roughness at 1.5D soil cover is shown in Fig. 17 (a) and Fig. 17 (b) shows the redrawn contour diagram. It was determined from these tests that the soil displacement behaviour is also similar to the displacement mechanism of Marston-Spangler's Projecting Type earth pressure theory regardless of the slope roughness and soil cover.

In this study, the earth pressure acting on the tunnel structure for soil cover with 1.0D and 1.50D was monitored at this size. The tendency of earth pressure of the surrounding soil to concentrate on the tunnel structure was due to the difference in the rigidity of the tunnel

1.0D-100 1.5D-100

(a) Soil Displacement Diagram

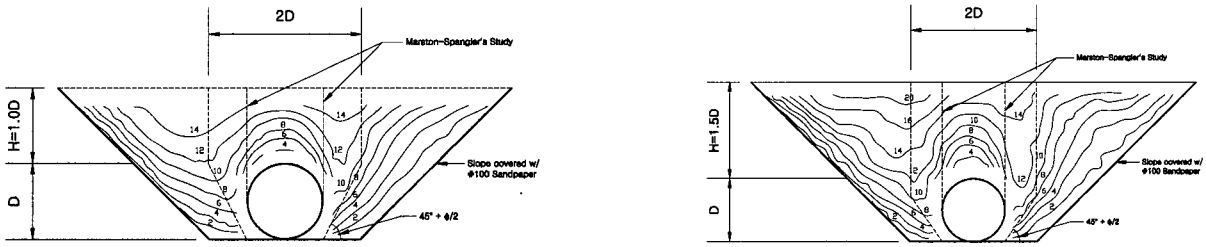

1.0D-100 1.5D-100

(b) Soil Displacement Countour

Fig. 16. Variation of Soil Behaviour with Soil Cover

1.5D-400 1.5D-ACE

(a) Soil Displacement Diagram

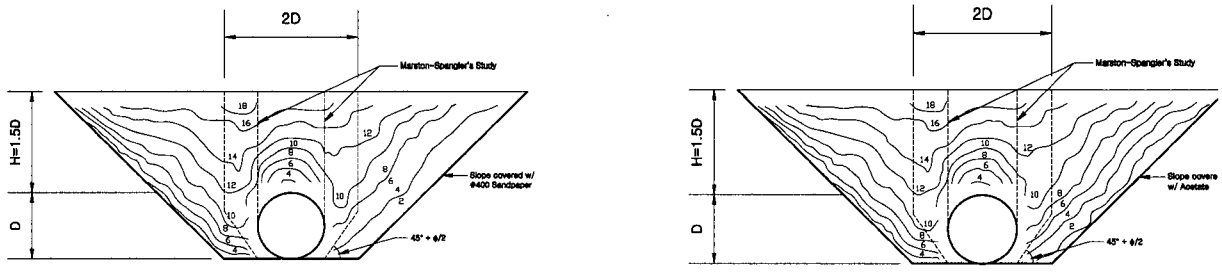

1.5D-400 1.5D-ACE

(b) Soil Displacement Countour

Fig. 17. Variation of Soil Behaviour with Slope Roughness

structure and the backfill soil. The relationship between this behaviour with the concrete and backfill soil at this size can only be determined through actual field testing. In the field, there will also be a large difference between the rigidity of the concrete lining and backfill soil at the tunnel portal. Furthermore, in work areas wherein the proper compaction of backfill material is not possible, Marston-Spangler's Projecting Type earth pressure theory may be used in the calculation of earth pressure.

4.2.2 Other Results

Results which include soil displacement vector, zero extension direction and maximum shear strain contour diagram are presented in Fig. 18 and Fig. 19. If we consider the maximum shear strain contour and zero extension direction diagram, it can be seen that failure

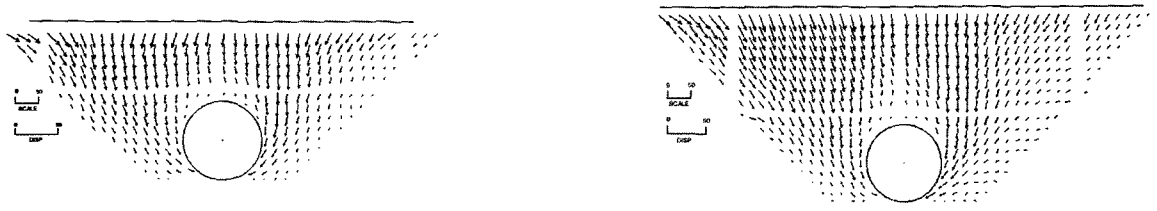

1.0D-100 1.5D-100

Soil displacement vector diagram

1.0D-100 1.5D-100

Zero extension direction diagram

1.0D-100 1.5D-100

Maximum shear strain contour diagram

Fig. 18. Picture Analysis Results of Soil Cover Variation

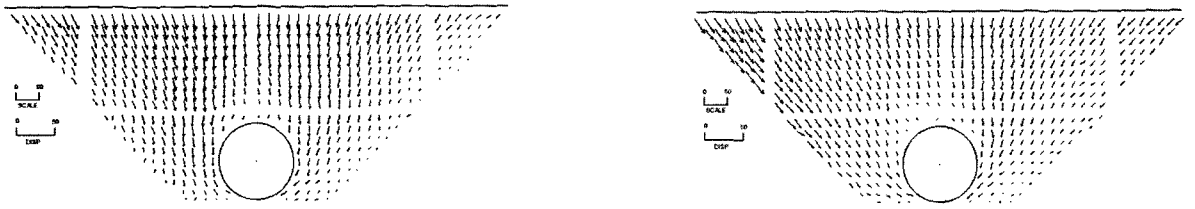

1.5D-400 1.5D-ACE

Soil displacement vector diagram

Fig. 19. Picture Analysis Results of Slope Roughness Variation

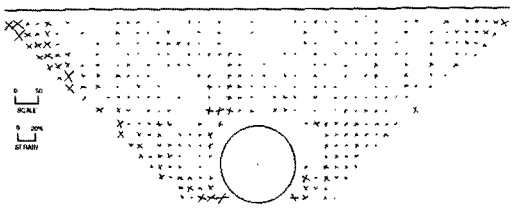

1.5D-400

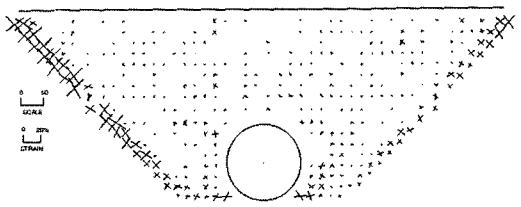

1.5D-ACE

Zero extension direction diagram

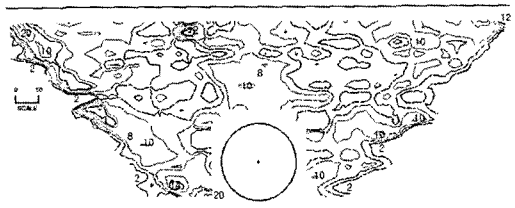

1.5D-400

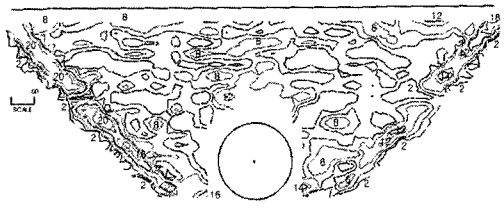

1.5D-ACE

Maximum shear strain contour diagram

Fig. 19. Picture Analysis Results of Slope Roughness Variation (continued)

surface occurs in the boundary between the original soil and backfill material. This can be seen in model tests with 1.0D and 1.5D soil cover. The failure surface can be clearly seen in the 1.5D-ACE.

5. Conclusion

In cut-and-cover tunnel construction, the compaction of the backfill material is the most important process, especially the backfill soil compaction on both sides of the tunnel. Even though the backfill material is properly compacted, several months or years after the construction is completed the backfill has the tendency to consolidate due to self-weight, precipitation and vibration caused by traffic. In the process, the tunnel is subjected to excessive earth pressure that causes the deformation and cracking of tunnel linings. These are classified as mechanical factors that cause tunnel damage. Damages can also be attributed to physical factors such as material properties and reinforcement corrosion, but in this study only damages due to mechanical factors in the form of additional loads were considered. Earth pressure acting on the tunnel lining generated by the backfill material and by its future settlement was investigated and analyzed through model test. In the model test the tunnel is rigid, the soil is loose and the vibration frequency used was 100 Hz.

Safety factor based on the difference between the monitored and computed earth pressure was recommended in order to prevent the damage of tunnel lining due to excessive earth pressure. The behaviour of soil around the tunnel lining obtained from the picture analysis was also presented. The conclusions obtained from this study can be summarized as follows:

(a) Existing earth pressure formulas has the tendency to underestimate the earth pressure acting on the tunnel lining.

(b) Judging from the magnitude of earth pressure acting on the tunnel crown and the shape of soil deformation around the tunnel, it can be seen that Marston-Spangler's Projecting Type Formula is the most applicable.

(c) Based on the analysis of soil deformation around the tunnel, it was determined that the extent of the additional load acting on the tunnel is much greater than the assumed width (D) in the Projecting Type Formula of Marston-Spangler's Theory. The width of additional load for tunnels with 1.0D and 1.5D soil cover was equivalent to twice the tunnel diameter

(2D).

(d) Application of Marston-Spangler's Projecting Type Formula requires the application of a safety factor equivalent to 1.3～1.5 for shallow tunnels with soil cover up to 1.5D.

(e) There is a need to perform more laboratory tunnel model tests in order to determine earth pressure reduction methods for excessive earth pressure acting on the cut-and-cover tunnel lining.

References

1. 김낙영, 이용준, 이승호, 정형식 (2002.12), "개착식 터널의 뒤채움재로 EPS블럭의 내진 성능 평가를 위한 진동대 시험", 한국터널공학회, *터널기술*, 제4권, 제4호, pp.333-342.
2. 김상윤 (2004), *개착식 터널의 라이닝에 작용하는 토압의 산정 및 경감대책에 관한 실험적 연구*, 부산대학교 석사학위논문.
3. 김은섭, 이상덕 (1999), "지하 박스구조물에 작용하는 토압에 관한 실험적 연구", *한국지반공학회논문집*, 제 15권, 제 6호, pp.235-246.
4. 고호성, 임종철, 박이근, 오명렬 (1996), "모래지반내의 터널굴착시 지반거동에 관한 실내모형실험", *대한 토목학회 학술발표 논문집*, pp.371-374.
5. 박이근 (2003.2), *얕은 토사터널 굴착시의 주변지반거동 특성과 마이크로 파일의 침하억제효과에 관한 연구*, 부산대학교 박사학위논문.
6. 윤건선 (1997), *실험 및 수치해석에 의한 복개터널 주위의 지압 및 터널 복공의 역학적 거동에 관한 연구*, 박사학위논문, 서울대학교 대학원.
7. 이대혁, 김영근, 이희근 (1998), "모형 실험에 의한 터널 복공의 역학적 거동 및 균열 특성에 관한 연구", *터널과 지하공간*, 한국암반공학회, 제8권, pp.53-66.
8. 林鍾鐵, 朴性栽, 朱仁坤, 朴鏞富, 金永仁 (1992), "平面變形率 狀態에 있는 模型地盤의 變形解釋法", *韓國地盤工學會誌* 第8卷 第1號, pp.29-39.
9. 임종철, 유문오, 박이근, 고호성, 오명렬 (2000.11), "터널 굴착시의 인접구조물 침하 억제용 마이크로파일의 효과에 관한 연구", *대한토목학회논문집*, 제20권, 6-C호, pp.565-577.
10. 임종철 외 6명 (2002.5), "토사 NATM 터널의 굴착에 의한 구조물 침하 억제대책 수립을 위한 실내모형실험 최종보고서", *삼성물산(주) 건설부문 및 부산대학교 생산기술연구소 공동연구*, pp.19-23.
11. 湯淺泰則 (1988), "土砂トンネルの力學的擧動に關する硏究", 京都大學 博士論文.
12. Adachi, T., Yashima, A. and Kojima, K. (1991), "Behaviour and simulation of sandy ground tunnels", *Developments in Geotechnical Aspects of Embankments, Excavations and Buried Structures, Balkema, Rotterdam*, pp.291-329.
13. Bierbäumer, A. (1913), *Die Dimensionnierung des Tunnelmanerwerks.*
14. Britto, A. M. (1979), *Thin walled buried pipes*, Doctorate Course Thesis, University of Cambridge.
15. Komiya, K., Shimizu, E., Watanabe, T. and Kodama, N. (2000), "Earth pressure exerted on tunnels due to the subsidence of sandy ground", *Geotechnical Aspect of Underground Construction in Soft Ground, Balkema, Rotterdam*, pp.397-402.
16. Konig, D., Gutter, G. U. and Jessberger, H. L. (1991), "Stress distribution during tunnel and shaft constructions", *Proc. International Conference, Centrifuge 91*, pp.129-135.
17. Nakai, T. and Zang, F. (1999), "Numerical simulation of excavation simulation in model tunnels", *34th Soil Engineering Conference*, pp.622-623.
18. Spangler, M. G. (1948), "Underground conduits - An appraisal of modern research", *Transactions of ASCE*, Paper No. 2337, Vol.113, pp.316-374.
19. Terzaghi, K. (1956), *Theoretical Soil Mechanics*, John Wiley & Sons, Inc., pp.69-76.

(접수일자 2005. 12. 7, 심사완료일 2006. 6. 13)